Journal of South American Earth Sciences, Vol. 2, No. 3, pp. 295–303, 1989
Printed in Great Britain

0895-9811/89 $3.00 + 0.00

Geochemistry and C–O isotopes of the Chiriguelo carbonatite, northeastern Paraguay

P. CENSI[1], P. COMIN-CHIARAMONTI[1], G. DEMARCHI[2], A. LONGINELLI[2], and D. ORUÈ[3]

[1]Istituto di Mineralogia, Petrografia e Geochimica, Università di Palermo, Italy;
[2]Istituto di Mineralogia e Petrografia, Università di Trieste, Italy;
[3]Instituto de Ciencias Bàsicas, Universidad Nacional de Asunción, Paraguay

(Received for publication April 1989)

Abstract—The Chiriguelo carbonatitic complex crops out in northeastern Paraguay at the central western fringe of the stratoid volcanic rock-types of the Serra Geral Formation. At least three stages of emplacement of carbonatitic rocks can be distinguished: a C1 main søvite, a C2 alvikite and a C3 ferrocarbonatite. A C4 stage may be inferred from the diffusion of late quartz, barite, and uranpyrochlore. The geologic, petrographic, and geochemical traits show environmental conditions similar to volcanic ones, and point to a vertical zonation in the fenitization processes versus a K-enrichment near the surface. The C–O isotopic data suggest a loss of isotopically light water, along with a loss of Sr, following the hydrothermal recrystallization process(es) of the main søvite. Such losses may be related to low-temperature (*e.g.* down to 25°C) weathering processes.

Resumo—O complexo carbonatitico de Chiriguelo aflora no nordeste do Paraguai associado a porção centro-oeste das rochas vulcânicas estratiformes da Serra Geral. Tal complexo é intrusivo em rochas precambrianas e paleozoicas. Ao menos tres estágios de intrusão carbonatítica podem ser observados: C1 constituido por søvito, C2 formado por alvikitos e C3 por ferrocarbonatitos. Um estágio C4 é inferido através da difusão de quartzo tardio, barita e uranopirocloro. As feções geológicas, geoquímicas e petrográficas mostram ambiente proximo á condições vulcânicas, e zoneamento vertical no processo de fenitização, onde ocorre enriquecimento de potassio em direção á superficie. O estudo isotopico de C e O sugere perda de agua isotopicamente leve depois do(s) processo(s) de recristalização do søvito C1, acompanhado(s) de perda de Sr. Tais perdas podem relacioner-se á diminução de pressão durante o estágio C4 e ão influxo de aguas meteoricas.

INTRODUCTION

THE CARBONATITIC COMPLEXES related to the Paraná Basin (South America) are located mainly north of the Rio Piquirí lineament (Fig. 1), and their ages range from 65 to 130 Ma (Rodrigues and dos Santos Lima, 1984). These complexes border the eastern, northeastern, and northern boundaries of the stratoid lavas of the Mesozoic Serra Geral Formation (Ulbrich and Gomes, 1981).

Several carbonatitic complexes crop out in Paraguay at the central-western border of the Paraná Basin (Premoli and Velasquez, 1981; Wiens, 1982; Haggerty and Mariano, 1983; Eby and Mariano, 1986), mainly in Amambay Province (Livieres and Quade, 1987). The age of the Chiriguelo Complex was determined by Eby and Mariano (1986) as between 119 and 126 Ma (fission tracks). Although some work has been carried out on the Chiriguelo Complex (*e.g.*, Grossi Sad, 1972; Berbert and Triquis, 1973; Haggerty and Mariano, 1983; Eby and Mariano, 1986), a systematic petrochemical and geochemical approach is not available; in particular, discussions regarding minor elements (such as Ba and Sr) in the carbonatites and the behavior of trace elements and stable isotopes (C–O) are lacking.

This paper presents an attempt to correlate geochemical characteristics with petrographic and geologic features, based on a study of samples collected from outcrops of the Chiriguelo Complex.

GEOLOGIC SETTING

The alkaline-carbonatitic body near the village of Chiriguelo was emplaced along a NE/SW-trending antiform lineament (Livieres and Quade, 1987). This circular structure, about 7.5 km in diameter, lies 25 km southwest of the town of P. J. Caballero-Ponta

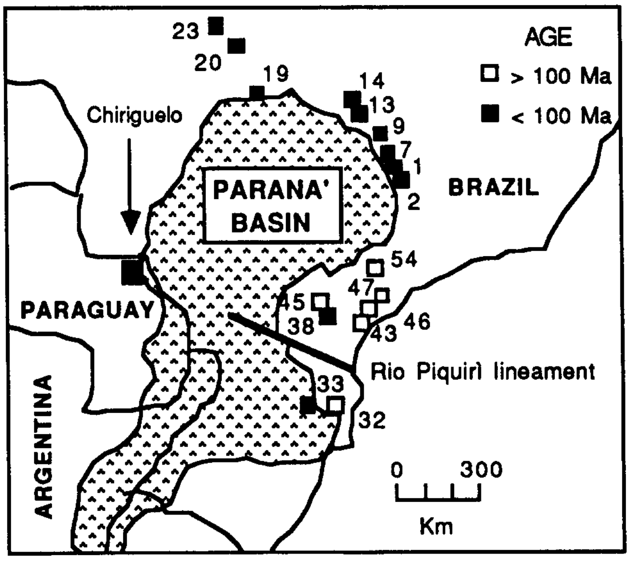

Fig. 1. Distribution of carbonatites with respect to the Paranà Basin. Numbers and age as in Rodrigues and dos Santos Lima (1984). The location of the Chiriguelo carbonatite is also shown.

Porá, between 22° 58' 45"S and 22° 39' 56"S and 55°54'07"W and 55°58' 45"W.

The complex intruded Precambrian metasediments, and peripheral country rocks show strong updoming. The southeastern limb is covered by late stratoid tholeiitic andesitic basalts of the Serra Geral Formation (Bellieni *et al.*, 1983, 1986). The main body of the carbonatitic rocks is a søvite (C1 stage, according to the nomenclature of Le Bas, 1977, 1980) that crops out in the central area of the complex and has an elliptical NE-SW form of about 600×300 meters (Fig. 2). The surrounding rocks are mainly breccias carrying abundant xenoliths of Precambrian basement. Massive fenites partially surround the brecciated area. Alvikitic veins (from 0.1 up to 10 cm wide: C2 stage) are scattered throughout the søvite, breccia, and fenite. Fenitic dikes (1-2 meters wide) and ferrocarbonatitic veins (1-20 cm wide: C3 stage) transgress the C1 and C2 carbonatites.

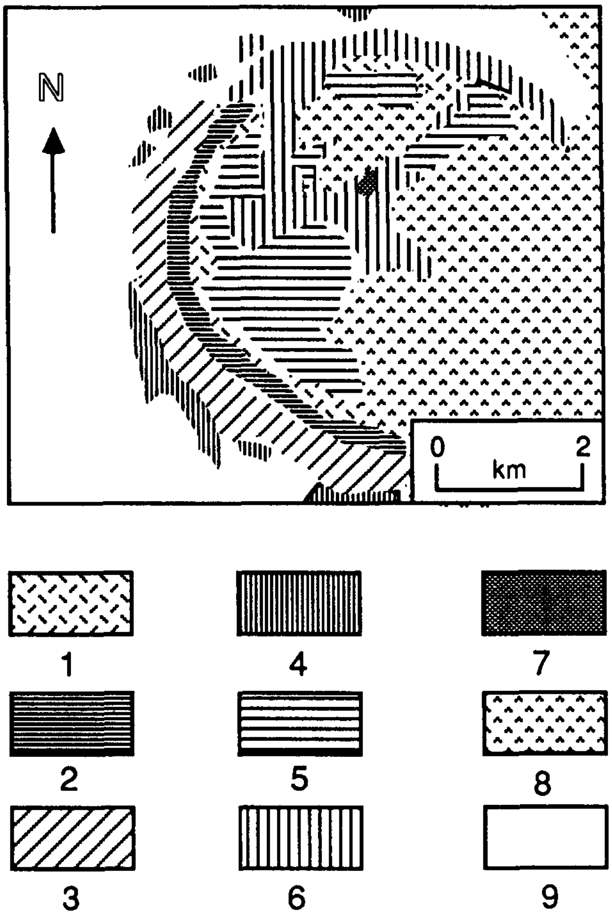

Fig. 2. Geological sketch map of the Ciriguelo Complex (Orué, unpublished survey): 1, Precambrian metasediments; 2, Silurian sediments; 3, Carboniferous sediments; 4, Mesozoic Misiones Formation; 5, massive fenite; 6, breccia; 7, main søvite; 8, stratoid volcanics of the Serra Geral Formation; 9, Quaternary sediments.

PETROGRAPHIC OUTLINES

Søvite

The søvite of the Chiriguelo Complex is light to medium grey and brown in color; its radioactivity is an average of 2 to 4 times background (Premoli and Velasquez, 1981). The texture of the søvite is usually subhedral-granular and medium to coarse grained; however, the range varies from a fine-grained "aplitic" texture to euhedral mosaics of extremely recrystallized calcite. Quartz, phlogopite, barite, sanidine (2Vx = 0-10°), apatite, dolomite, uranpyrochlore, magnetite, aegirine, zircon, strontianite, synchysite, hematite, goethite, pyrite, and other minerals may be present. Quartz and barite appear as late phases along the uranpyrochlore, filling fractures and intergranular spaces.

Temperatures of equilibration, based on calcite-$MgCO_3$ content (Rice, 1977; Gittings, 1979), show a range from 200°C for coarse recrystallized rock-types, to 450°C for rock-types having a tendency toward aplitic textures. However, the reliability of this geothermometer is rather poor and, in any case, only indicates re-equilibration temperatures. The presence of sanidine and phlogopite indicates that emplacement temperatures were in fact considerably higher than those inferred by the calcite-$MgCO_3$ equilibration and substantially near-surface volcanic conditions (*cf.* Le Bas, 1980).

Breccias and Massive Fenites

The breccias are formed of basement xenoliths (mainly quartzites and meta-arkoses), autoliths (trachytic aggregates of sanidine, quartz, and aegirine), carbonatitic fragments, sanidine clasts, aegirine, and sanidine mircophenocrysts embedded in a very fine-grained limonitic matrix. The brecciation was probably caused by H_2O and CO_2 release associated with søvite crystallization.

Massive fenites have a porphyritic texture and a trachytic composition, with phenocrysts of sanidine and mircophenocrysts of sanidine, aegirine, biotite, and magnetite set in a groundmass consisting of the same phases, plus glass and goethite-limonite patches.

Alvikites, Ferrocarbonatites, and Fenitic Dikes

The alvikites are usually very fine grained and have an aplitic texture, with chilled margins showing evidence of flow parallel to the walls (microboudins). Quartz, phlogopite, apatite, hematite, and suphides are present.

The ferrocarbonatites are normally composed of ferroan calcite rhombohedra that have cores containing opaque iron oxide. Goethite and limonite surround the calcite crystals. Clusters of apatite, sanidine, and phlogopite occur, as well as carbonatitic fragments similar to the C1 søvite (main søvite).

The fenitic dikes have a trachytic composition and show a weak porphyritic hypocrystalline texture, with phenocrysts and microphenocrysts of sanidine set in a groundmass consisting of glass, sanidine, aegirine, opaques, and accessory apatite. Completely altered euhedral crystals can be found, which could be relicts of garnet crystals.

ANALYTICAL PROCEDURES

Samples intended for chemical analyses were reduced in an agate disc mill and dried at 110°C. The major and trace elements were determined on a Philips PW1401 X-ray spectrometer with full matrix correction, according to the methods of Franzine *et al.* (1975) and Leoni and Saitta (1976). Ca and Mg analyses were repeated by volumetric EDTA titration. Ignition losses (LOI) were determined at 1000°C and controlled for CO_2 content following the standard wet chemical procedures.

Accuracy was monitored by international standards. The precision for major and minor elements (including Ba and Sr) is better than 2%. The precision for Cr, Ni, Rb, Nb, (Ba and Sr) trace elements is better than 10% and 20% for contents >20 ppm and <20 ppm, respectively; the precision for La, Ce, Nd and Zr is better than 10%; the precision for U, Th, Sm, Yb, and Y results better than 30% and 50% for contents >20 ppm and <20 ppm, respectively.

The samples were finally prepared for the analysis of isotopic composition by vacuum heating at 400° C and reacting with 100% H_3PO_4, according to well-known precedures.

Isotopic analyses were performed with a FINNIGAN Mat Delta E mass spectrometer and the results are given in terms of usual δ‰ units.

Reference standards are PDB-1 and V-SMOW for C and O isotopic composition, respectively. The standard deviation of the entire analytical precedure is about ±0.05‰ (1σ) for both carbon and oxygen.

GEOCHEMISTRY

Selected analyses representing the described rock-types of the Chiriguelo complex are reported in Table 1.

Compared to the average carbonatite composition given by Gold (1966), the Chiriguelo søvite has a low content of Fe, Mg, and Na and a high content of Ca and Ba. The average K_2O/Na_2O and Ba/Sr ratios of these rocks are, respectively, 4.43 and 5.65 (excluding søvite, sample 7, which includes abundant sanidine, and sample 10, which is a completely recrystallized søvite); The same ratios reported by Gold (1966) for average carbonatites are, respectively, 0.80 and 0.53. Alvikites and ferrocarbonatites have K_2O/Na_2O and Ba/Sr ratios of 3.00 and 1.12 and of 53.7 and 3.08, repectively. The Nb, U, and Th content of these rocks appears to be related to the local abundance of uranpyrochlore.

The associated fenitized rocks (breccias, massive fenites, and fenitic dikes) display stronger enrichment of K (up to 11.71% wt) than Na_2O (up to 1.50% wt), suggesting a parental K-rich magma that produced an alkali carbonate fraction by liquid immiscibility (Wooley, 1982; Kasputin, 1983). Alternatively the K-rich fenites could reflect vertical zonation (Le Bas, 1980) where the sodic fenites reflect deeper levels and the potassic fenites represent shallow levels (*cf.* Wooley, 1982).

In general, carbonatites related to a K-rich parent liquid are enriched in REE and have higher values of LREE/HREE ratios than those of the sodic series (Samoylov and Smirnova, 1980). In the La/Yb *vs* La diagram (Fig. 3), the Chiriguelo carbonatites plot into the generalized carbonatite field (*cf.* Andersen, 1987) and fall in an area between the potassic and sodic carbonatites. The REE pattern of the Chiriguelo main søvite, normalized to chondrites, shows an enrichment of LREE with respect to the sodic carbonatites (Fig. 4A and B). The fenitic rock-types display enrichment mainly in Sm, Yb (Fig. 4C), and Y (*cf.* Table 1), and the breccia has the highest REE contents. The recrystallized søvite 10 that parallels the behavior of the main søvite, has the lowest REE content (Fig. 4A). The søvite with the highest Nb and U content (*cf.* analysis 1 of Table 1) points to a relative enrichment in Sm with respect to the main søvite, which suggests a possible selective "contamination" by a later carbonatitic emplacement (stage C4?).

The following brought us to surmise that a later stage (C4) was a possible source of the change in the original contents of the main trace elements, thereby favoring the late formation of the sulphate, quartz, and uranpyrochlore phases (*cf.* Le Bas, 1980, 1987; Kasputin, 1983): (1) the presence of quartz, barite, and uranium minerals in the main sôvite; (2) the higher content of Ba with respect to Sr; (3) the almost constant ratio between REE and BA (REE/Ba=0.12 ±0.02), showing a direct link between REE and $BaSO_4$ phase.

Probably the combined effects of vertical zonation and of superimposed fenitization processes (belonging to the various stages of emplacement of the carbonatites (*i.e.*, C1 to C4) are responsible for the mixed characteristics falling between the "sodic" and "potassic" carbonatite fields (Fig. 3).

ISOTOPIC DATA

The C and O isotopic compositions for carbonatitic rock-types of the Chiriguelo Complex are reported in Table 2, in the δ notations, as $\delta^{13}C$ *vs* PBD-1 and $\delta^{18}O$ *vs* V-SMOW, respectively. These results are shown graphically in Fig. 5.

The $\delta^{13}C$ values range from −3.97 to −8.08, while the $\delta^{18}O$ values display a very strong increase throughout the same sequence, ranging from +11.22 to +22.91.

Table 1. Representative chemical analyses of the Chiriguelo Complex.

	1	2	3	4	5	6	7	8	9	10
	3443	3434	3422	3420	3414	3411	3436	3409	3435B	3442
SiO_2	6.25	7.18	5.05	2.31	5.44	2.26	8.70	2.31	5.74	3.28
TiO_2	0.30	0.10	0.10	0.06	0.05	0.05	0.18	0.06	0.22	0.04
Al_2O_3	0.53	0.56	0.30	0.26	0.25	0.22	1.47	0.24	0.25	0.09
Fe_2O_3*	4.34	3.32	3.54	3.49	3.16	3.61	3.21	2.31	1.72	1.84
MnO	0.40	0.15	0.28	0.17	0.45	0.60	0.21	0.30	0.26	0.14
MgO	1.00	0.50	0.41	0.15	0.15	0.10	0.67	0.13	0.15	0.05
CaO	44.62	46.98	47.00	49.25	47.15	48.45	44.43	50.03	50.75	50.68
BaO	2.15	1.16	2.47	2.60	2.79	2.89	1.24	2.98	1.14	0.64
SrO	0.84	0.88	0.57	0.37	0.25	0.34	0.77	0.49	1.08	1.53
Na_2O	0.10	0.04	0.03	0.09	0.08	0.08	0.05	0.05	0.09	0.09
K_2O	0.42	0.50	0.28	0.13	0.15	0.07	1.39	0.13	0.27	0.07
P_2O_5	1.20	0.48	0.69	0.88	0.95	0.80	0.52	0.48	0.42	0.45
LOI	37.08	38.05	38.29	39.62	38.07	38.99	36.29	40.46	40.78	40.61
Total	99.23	99.90	99.01	99.39	98.95	98.46	99.16	99.97	99.59	99.51
La	889	590	1169	1016	1257	1336	491	1546	1028	321
Ce	1022	633	1102	947	1240	1305	653	1619	904	362
Nd	151	120	178	133	181	215	153	309	117	59
Sm	94	20	30	28	33	21	15	36	18	6
Yb	9	6	8	10	13	8	4	11	8	<4
Y	5	10	<4	<4	<4	<4	8	5	11	<4
Cr	3	6	10	16	4	9	46	10	48	0
Ni	5	9	16	7	17	19	15	17	18	2
Rb	59	36	39	36	32	24	73	31	58	16
Ba	19532	10390	22123	23287	23989	25885	11106	26691	24810	5732
Nb	4951	10	178	18	81	109	65	80	124	99
Sr	7103	7441	5243	3129	2031	2875	6511	4158	4397	12938
Zr	39	430	219	146	87	133	840	165	243	1137
U	590	nd	22	nd	nd	nd	nd	nd	15	nd
Th	12	nd	10	nd	nd	nd	nd	nd	nd	nd

Key: 1–9, the main søvite; 10, recrystallized søvite; 11 and 12, breccia; 13–15, massive fenite; 16, alvikite; 17, ferrocarbonatite; 18 and 19, fenitic dikes; 20, average of carbonatites (Gold, 1966).

*Total iron as Fe_2O_3; nd, not determined.

Taylor *et al.* (1967) noted that the probable field of primary carbonatites has $\delta^{13}C$ and $\delta^{18}O$ ranging from −4.9 to −8.0 and +6.0 to +8.8 respectively.

The whole regression $\delta^{13}C$ *vs* $\delta^{18}O$ line (Fig. 5), relative to the carbonatite samples, shows a slope of 0.31 (r = 0.858). This trend is similar to that expected from a Rayleigh distillation model of fractionation between the crystallizing calcite and the coexisting vapor phase at 700°C having H_2O/CO_2 molar ratios between 0.4 and 0.5 in a closed system (equations in Pineau *et al.*, 1973). It is notable in this model that, for temperatures lower than 400°C, the slope of the path strongly decreases down to negative values and that the initial isotopic composition does not affect the slope of the path, which can be transferred to any appropriate starting composition.

Figure 5 shows two possible paths from starting compositions of $\delta^{13}C$ - $\delta^{18}O$: path 1 has −7.5 and +7, and path 2 has −8.5 and +8 $\delta^{13}C$ and $\delta^{18}O$, repectively. The two paths roughly give the idea that two carbonatitic types have almost equilibrated at decreasing temperatures in a closed system, starting from magmatic conditions. However, there are some constraints on the above model — in particular:

1. The field characteristics as well as the petrographical and petrochemical features of the main søvite do not show evidence of more than one parent source.
2. If the entire $\delta^{13}C$ range relative to the main søvite (−3.97 to −8.08) roughly corresponds to the isotopic composition estimated for the mantle-derived carbon ($\delta^{13}C = -2$ to -8 according to Hoefs, 1973, with $\delta^{13}C$ around −7 as a probable value according to Javoy *et al.*, 1986), the oxygen isotope composition is quite out of the range expected for materials produced from mantle sources through distillation processes (*e.g.*, initial $\delta^{18}O = +7$ *vs* final +17 according to Pineau *et al.*, 1973).
3. Among the main søvite samples, the completely recrystallized søvite 10 is the sample that better approaches the starting composition of path 1 (Fig. 5). However, in a fractionation model where tem-

Table 1 (continued)

	11 3429	12 3430	13 3427	14 3426	15 3431	16 3435A	17 3440	18 3423	19 3424	20 avg
SiO_2	68.07	66.38	57.02	57.99	59.11	2.46	10.55	55.24	56.93	5.67
TiO_2	1.39	1.47	1.19	1.03	1.35	0.22	3.41	1.34	1.11	0.50
Al_2O_3	7.70	5.19	15.16	15.07	12.67	0.25	1.44	17.63	16.96	1.77
Fe_2O_3*	10.94	10.45	8.64	7.96	12.29	1.72	15.20	8.86	8.87	8.00
MnO	0.28	0.17	0.21	0.20	0.58	0.26	0.64	0.37	0.25	0.78
MgO	0.76	0.72	2.28	1.65	1.10	0.90	2.80	1.12	0.65	6.10
CaO	2.12	3.13	0.82	0.62	0.06	50.00	30.89	0.28	0.19	37.06
BaO	0.70	3.95	0.43	0.47	0.20	1.14	0.61	0.50	0.34	0.45
SrO	0.05	0.05	0.09	0.10	0.00	1.08	0.21	1.06	0.06	0.89
Na_2O	0.08	0.17	1.50	1.48	0.03	0.09	0.03	0.26	0.20	1.09
K_2O	3.53	2.68	10.41	11.71	11.06	0.27	1.61	11.61	12.53	0.87
P_2O_5	0.63	0.70	0.28	0.27	0.05	0.42	0.54	0.06	0.08	1.73
LOI	3.50	4.85	1.90	1.46	1.70	40.78	31.12	2.27	2.23	33.58
Total	99.75	99.91	99.93	100.01	100.20	99.59	99.05	99.60	100.40	98.49
La	2422	2503	919	730	300	565	312	813	622	
Ce	2501	2443	625	605	540	611	227	733	489	
Nd	833	717	459	430	127	124	110	405	358	
Sm	230	210	128	105	40	20	12	113	91	
Yb	130	109	19	12	<4	5	4	8	7	
Y	141	152	98	204	14	9	29	156	144	
Cr	101	74	16	14	13	21	461	45	20	102
Ni	14	14	9	10	8	15	38	12	11	32
Rb	128	91	233	247	178	39	151	218	256	52
Ba	6246	35378	3881	4223	1771	10221	5464	4478	3069	4031
Nb	428	329	109	86	528	15	260	138	124	560
Sr	452	445	765	839	85	9133	1776	543	543	7526
Zr	299	260	591	748	44	532	506	870	598	641
U	27	18	14	6	71	nd	9	5	5	
Th	58	61	47	26	166	nd	8	38	25	

Key: 1–9, the main søvite; 10, recrystallized søvite; 11 and 12, breccia; 13–15, massive fenite; 16, alvikite; 17, ferrocarbonatite; 18 and 19, fenitic dikes; 20, average of carbonatites (Gold, 1966).

*Total iron as Fe_2O_3; nd, not determined.

peratures decrease, the søvite 10 should plot in a more evolved region of the trend. The observed isotopic values for søvite 10 are more in agreement with a recrystallization induced by temperatures lower than 400°C (*e.g.*, 200°C, *cf.* Pineau *et al.*, 1973).

4. In a fractionation model from high to late magmatic temperatures the ^{18}O and ^{13}C enrichment parallels a REE enrichment (Loubet *et al.*, 1972). The REE behavior of the Chiriguelo carbonatites with respect to the ^{18}O and ^{13}C enrichment seems to point to a positive correlation for some samples (1, 2, 3, 7, 8 of Table 2, corresponding to the middle part of path 2 in Fig. 5), but the main correlation seems to be negative (Fig. 6) — also because the probable REE redistribution is linked to the late sulphate-rich phase(s) of the C4 stage.

In general the interpretation of the C and O isotope compositions is difficult because of the readiness with which calcite re-equilibrates; all the values plotted out of the field outlined by Taylor *et al.* (1967) should correspond with rock-types that re-equilibrated at variable temperatures relative to both hydrothermal fluids and metoric waters (Pineau *et al.*, 1973).

According to Deines and Gold (1973) and to Nielsen and Buchard (1985), the spreading from low to high δ^{18}O and δ^{13}C values is correlated to near-surface emplacement (volcanic-subvolcanic associations), as opposed to the subvolcanic intrusive types. Furthermore, Deines and Gold (1973) advanced three main arguments to explain the occurrence of comparatively high δ^{18}O values in shallow carbonatites: loss of isotopically light water by pressure release during emplacement; re-equilibration of calcite with magmatic carbonatite water to low temperatures; and influx of meteoric waters.

In the latter case, any isotope exchange would have to be limited to temperatures lower than 250°C, because at higher temperatures an exchange with surface or ground waters (δ^{18}O < 0‰) would lead to a depletion in ^{18}O. In fact, when calcite from carbonatites is affected by isotopic exchange during hydro-

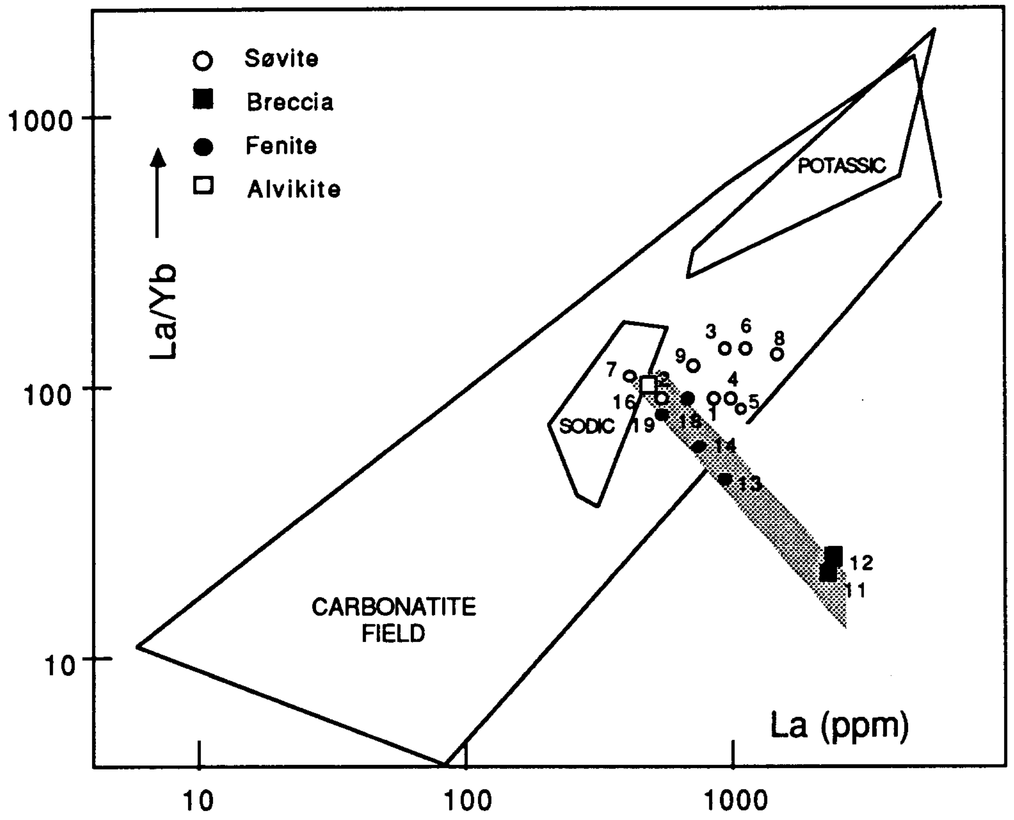

Fig. 3. La/Yb *vs* La for the rock types of the Chiriguelo Complex: carbonatite field from Andersen (1987); sodic and potassic fields from Samoylov and Smirnova (1980). Dashed area is field of fenitized rock types in the Chiriguelo Complex; sample numbers as in Table 1.

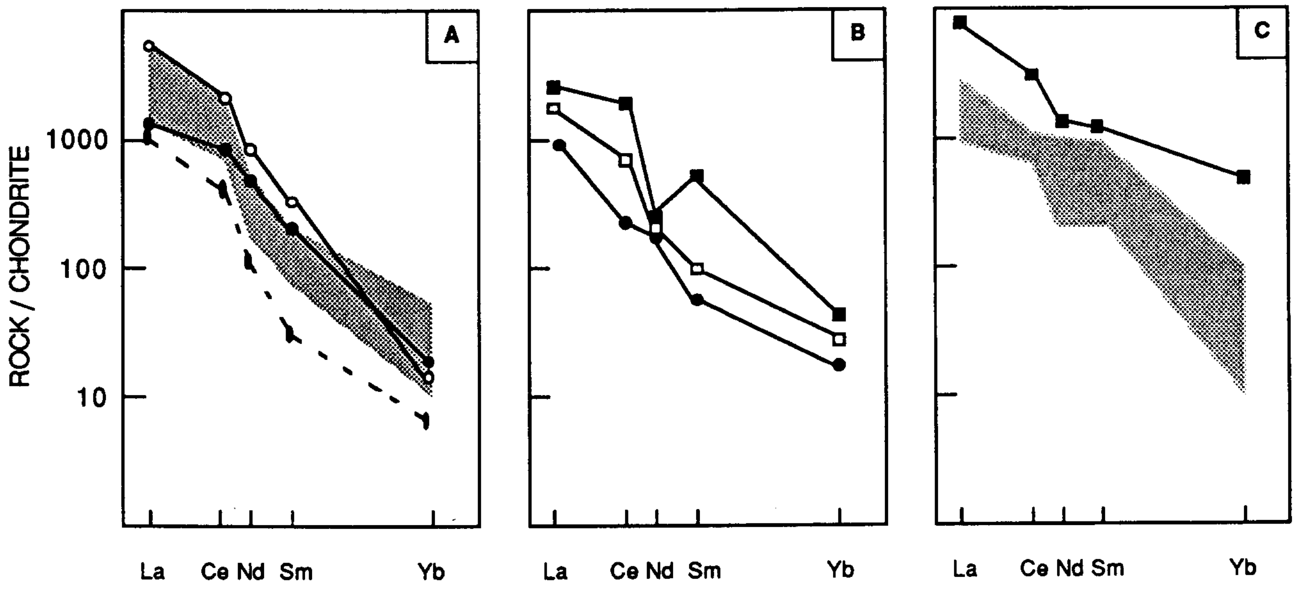

Fig. 4. REE normalized to chondrites (*Chrondrites* values from Taylor and Gorton, 1977) for the Chiriguelo rock types. A, dotted area represents the field of the main søvite; bars represent the behavior of the recrystallized søvite 10; solid circles, sodic søvite pattern; open circles, potassic søvite pattern (inferred from Samoylov and Smirnova, 1980). B, Solid squares, unranpyrochlore carbonatite 1; open squares, alvikite 16; solid circles, Fe-carbonatite 17. C, dotted area represents the whole pattern relative to fenites (both massive fenite and dikes) of the Chiriguelo Complex; solid squares, fenitized breccia.

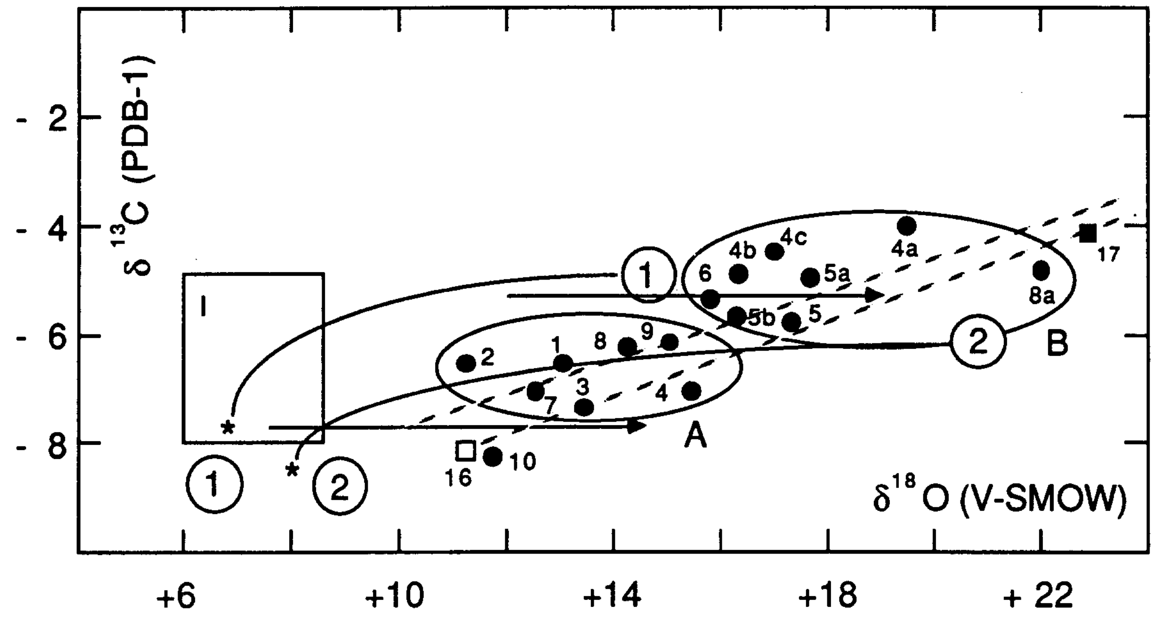

Fig. 5. δ^{13}C *versus* δ^{18}O for the Chiriguelo carbonatitic samples: solid circles, main søvite (see text for A and B fields); open square, alvikite; solid square, Fe-carbonatite; I, "box" of primary carbonatites (Taylor *et al.*, 1987); 1 and 2, isotopic fractionation paths (Pineau *et al.*, 1973) transferred to arbitrary starting compositions (asterisks). Dashed lines represent the regression lines for the analyzed samples. The lines with arrows indicate the paths of possible weathering effects; sample numbers as in Table 1.

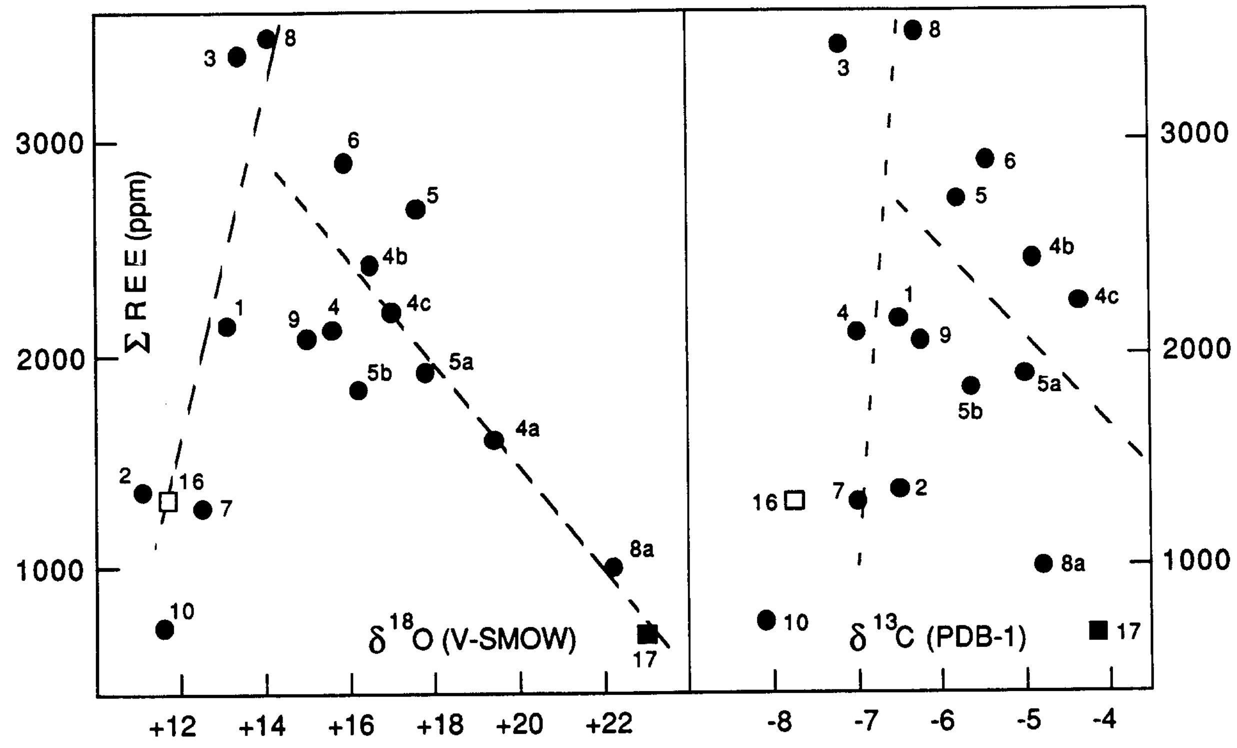

Fig. 6. Relationships between C–O isotopic compositions and ΣREE (ppm) in the Chiriguelo carbonatitic samples: solid circles, main søvite; open square, alvikite; solid square, Fe-carbonatite; sample numbers as in Table 1.

Table 2. Selected analyses of the isotopic composition of Chiriguelo carbonatitic samples. ΣRee (ppm) are also reported.

n°	Sample	$\delta^{13}C$ vs PDB-1	$\delta^{18}O$ vs V-SMOW	ΣRee (ppm)
1	3443	−6.49	+13.07	2165
2	3434	−6.52	+11.22	1369
3	3422	−7.26	+13.48	3422
4	3420	−6.98	+15.45	2134
4a	3419	−3.97	+19.44	1599
4b	3417	−4.98	+16.38	2415
4c	3416	−4.40	+17.10	2210
5	3414	−5.75	+17.56	2724
5a	3412	−4.98	+17.76	1926
5b	3413	−5.80	+16.21	1832
6	3411	−5.48	+15.93	2885
7	3436	−7.07	+12.51	1316
8	3409	−6.30	+14.14	3521
8a	3410	−4.71	+22.33	1000
9	3435B	−6.25	+14.94	2075
10	3442	−8.08	+11.76	748
16	3435A	−7.77	+11.53	1325
17	3440	−4.10	+22.91	655

thermal, deuteric, or weathering events, its oxygen isotope composition generally increases, while $\delta^{13}C$ remains roughly the same (Pineau *et al.*, 1973).

Considering $\delta^{13}C$ enrichment, however, two groups belonging to the main søvite are apparent in Fig. 5 (excluding sample 10):

A) samples with average $\delta^{13}C = -6.70 \pm 0.40‰$ and with $\delta^{18}O$ ranging from +11.22 to +15.45‰; and
B) samples with average $\delta^{13}C = -5.01 \pm 0.65‰$ and with $\delta^{18}O$ ranging from +15.93 to +22.33‰.

These features, which lack evidence of different parent sources, should represent two different low-temperature trends that should start from different isotopic compositions and should also belong to different stages of the fractionation (s. path 1 of Fig. 5) and emplacement processes.

Based on the foregoing, the following model can be proposed:

- Emplacement at shallower levels of a carbonatitic magma evolving via a distillation path (*e.g.*, path 1 of Fig. 5), roughly up to a $\delta^{18}O$ value around +8.5 and $\delta^{13}C$ around −6.5‰.
- Re-equilibration of the søvite 10 at hydrothermal conditions that caused a depletion in $\delta^{13}C$.
- Weathering of Group A samples.
- Vapor escape during emplacement and shifting of $\delta^{18}O$ and $\delta^{13}C$ *vs* more positive values (source for Group B samples).
- Weathering of Group B samples at very low temperature (*e.g.*, 25°C).

Alvikites and Fe-carbonatites could conceivably represent hydrothermal and extreme weathering conditions, respectively.

The model is supported by the behavior of Sr *vs* $\delta^{18}O$ (Fig. 7), which shows an exponential correlation (diffusion process type), where the samples belonging to Group B display the lowest Sr content. The $\delta^{18}O$ value measured for recrystallized søvite 10 fits "perfectly" with the calculated exponential curve. This means that any loss of isotopically light water and Sr should be attributed to a later stage than the isotopic re-equilibration of søvite 10. In fact, assuming that recrystallization of søvite 10 occurred at hydrothermal conditions in an environment having a Sr content corresponding to the equilibrium concentrations of carbonatite solution (Pineau *et al.*, 1973), the Sr loss occurring in the other carbonatite samples is interpreted here as the consequence of the interactions between carbonatite and solutions with much lower Sr contents (*i.e.*, meteoric weathering conditions).

SUMMARY AND CONCLUSIONS

The Chiriguelo carbonatitic complex was emplaced as a sanidine-calcite facies close to volcanic conditions. Femic rock-types corresponding to possible primary melts, or to poorly evolved ones, were not encountered in the field. The magmatic rock-types associated with the carbonatite are fenitized and trachytic in composition, with strong potassic affinity.

In spite of the potassic affinity, indicated by the fenitic rock-types, the geochemical features may be referred to a parental sodic source that underwent vertical zonation during the fenitization process(es) (potassic imprinting of the sampled shallow levels).

At least three carbonatitic stages can be distinguished: C1 main søvite; C2 alvikite; and C3 ferrocarbonatite. A C4 stage is proposed because of the late emplacement of barite, quartz, and uranpyrochlore.

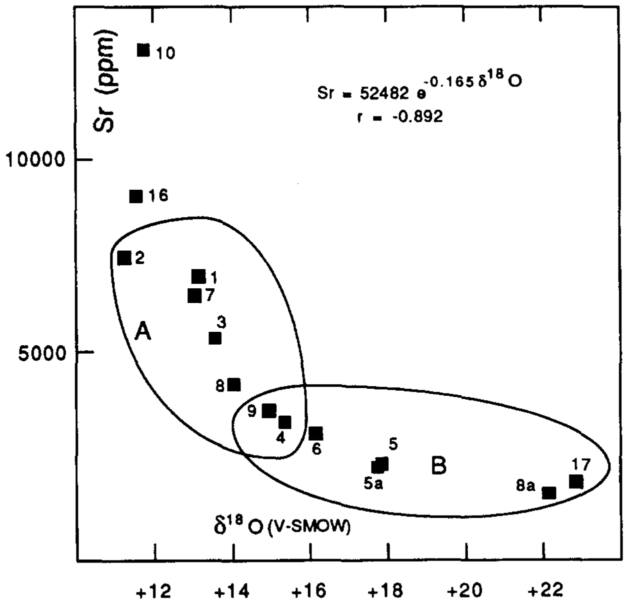

Fig. 7. Sr *vs* $\delta^{18}O$ in the carbonatite of the Chiriguelo Complex; sample numbers as in Table 1.

The $\delta^{18}O$ - $\delta^{13}C$ isotopic data suggest that the ^{18}O isotopic enrichment took place after the hydrothermal re-equilibration of the carbonatite and may be related to late influx of meteoric waters at very low temperature conditions.

Acknowledgements—The manuscript was substantially improved by constructive criticism by K. Bell. The authors wish to express their thanks to MPI (Italian agency) and to CNPq, FAPESP, FINEP (Brazilian agencies) for financial support.

REFERENCES

Andersen, T., 1987. Mantle and crustal components in a carbonatite complex, and the evolution of carbonatite magma: REE and isotopic evidence from the Fen complex, southeast Norway. *Isotope Geoscience* **65**, 147-166.

Bellieni G., Brotzu, P., Comin-Chiaramonti, P., Ernesto, M., Melfi, A. J., Pacca, I. G., Piccirillo, E. M., and Stolfa, D., 1983. Petrological and paleomagnetic data on the plateau basalt to rhyolite sequences of the Southern Paraná Basin (Brazil). *Anais da Academia Brasileira de Ciencias* **55**, 355-383.

Bellieni, G., Comin-Chiaramonti, P., Marques, L. S., Melfi, A. J., Nardy, A. J. R., Papatrechas, C., Piccirillo, E. M., Roisemberg, A., and Stolfa, D., 1986. Petrogenetic aspects of acid and basaltic lavas from the Paraná Plateau (Brazil): Geological, mineralogical and petrochemical relationships. *Journal of Petrology* **27**, 915-944.

Berbert, C., and Triquis, G., 1973. Carbonatito de Pedro Juan Caballero, Paraguay. *Congresso Brasileiro de Geologia* **27**, 77-78.

Deines, P., and Gold, D. P., 1973. The isotopic composition of carbonatite and kimberlite carbonates and their bearing on the isotopic composition of deep-seated carbon. *Geochimica Cosmochimica Acta* **37**, 1709-1733.

Eby, N. G., and Mariano, A. N., 1986. *Geology and Geochronology of Carbonatites Peripheral to the Paraná Basin, Brazil-Paraguay.* Carbonatites Symposium, Ottawa, 13 p.

Franzini, M., Leoni, L., and Saitta, M., 1975. Revisione di una metodologia analitica per fluorescenza-X basata sulla correzione degli effetti di matrice. *Rendiconti della Società Italiana di Mineralogia e Petrologia* **31**, 365-378.

Gittings, J., 1979. Problems inherent in the application of calcite-dolomite geothermometry to carbonatites. *Contributions to Mineralogy and Petrology* **69**, 1-4.

Gold, D. P., 1966. The minerals of the Oka carbonatite and alkaline complex, Oka, Quebec. In: *Proceedings, VI General Meeting of the International Mineral Association, India*, 109-125.

Grossi Sad, J. H., 1972. *Relatorio Preliminar Sobre as Possiblitades Minerals do Complexo Igneo de Chiriguelo em Pedro Juan Caballero.* GEOSOL. Belo Horizonte, 42 p.

Haggerty, S. E., and Mariano, A. N., 1983. Strontian loparite and strontio-chevkinite: tow new minerals in rheomorphic fenites from the Paraná Basin carbonatites, South America. *Contributions to Mineralogy and Petrology* **84**, 365-381.

Hoefs, J., 1973. Ein Beitrag zur Isotopen Geochemie des Kohlenstaffs in magmatischen Gesteinen. *Contributions to Mineralogy and Petrology* **41**, 277-300.

Javoy, M., Pineau, F., and Delorme, H., 1986. Carbon and nitrogen isotopes in the mantle. *Chemical Geology* **57**, 41-62.

Kasputin, Y. L., 1983. Stontium and barium geochemistry in carbonatite complexes. *Geokhimiya* **7**, 931-944.

Le Bas, M. J., 1977 *Carbonatite-Nephelinite Volcanism: An African Case History.* J. Wiley and Sons, New York, 347 p.

Le Bas, M. J., 1981. Carbonatite magmas. *Mineralogical Magazine* **44**, 133-140.

Le Bas, M. J., 1987. Nephelinites and carbonatites. In: *Alkaline Igneous Rocks* (Edited by J. G. Fitton and B. G. Y. Upton). Geological Society of Edinburgh, Specical Publication **30**, 53-83.

Leoni L., and Saitta, M., 1976. X-ray fluorescence analysis of 29 trace elements in rock and mineral standard. *Rendiconti della Società Italiana di Mineralogia e Petrologia* **32**, 497-510.

Loubet, M., Bernat, M., Javoy, M., and Allegre, C. J., 1972. Rare earth contents in carbonatites. *Earth and Planetary Science Letters* **14**, 226-232.

Nielsen, T. F. D., and Buchardt, B., 1985. Sr–C–O isotopes in nephelinitic rocks and carbonatites, Gardiner complex, Tertiary of East Greenland. *Chemical Geology* **53**, 207-217.

Pineau, F., Javoy, M., and Allegre, C. J., 1973. Étude systématique des isotopes de l'oxigène du carbon et du strontium dans les carbonatites. *Geochimica Cosmochimica Acta* **37**, 2363-2377.

Premoli, C., and Velazquez, J. C., 1981. Preliminary reconnaissance for uranium in Paraguay. *International Atomic Energy Agency, Vienna* **162** (20), 373-394.

Rice, Y. M., 1977. Contact metamorphism of impure dolomitic limestone in the Bouldero aureole, Montana. *Contributions in Mineralogy and Petrology* **59**, 237-259.

Rodrigues, C. S., and Santos Lima, P. R. A., 1984. *Carbonatitic Complexes of Brazil.* Companhia Brasileira de Metalurgia e Minerazão, Sao Paulo, 3-17.

Samoylov, V. S., and Smirnova, Y. V., 1980. Rare-earth behavior formation and the origin of carbonatites. *Geokhimiya* **12**, 1844-1858.

Taylor, H. P., Jr., Frechen, J., and Degens, E. T., 1967. Oxygen and carbon isotope studies of carbonatites from the Laacher See district, West Germany and Alno district, Sweden. *Geochimica Cosmochimica Acta* **31**, 407-430.

Taylor, S. R., and Gorton, M. P., 1977. Geochemical application of spark source mass spectrography: III, Element sensitivity, precision and accuracy. *Geochimica Cosmochimica Acta* **41**, 1375-1380.

Ulbrich, H. H. G. J., and Gomes, C. B., 1981. Alkaline rocks from continental Brazil. *Earth Science Reviews* **17**, 135-154.